

2D X-ray spectrometer on WEST: diffracting crystal study and first temperature profiles

A. Da Ros¹, D. Vezinet¹, G. Colledani¹, F. Bombarda², V. De Leo² and the WEST Team³

¹ CEA, IRFM, F-13108 Saint Paul-lez-Durance, France

² ENEA-FSN, Frascati (Rome), Italy

³ See (<http://west.cea.fr/WESTteam>) for the WEST Team

Abstract: The influence of Bragg crystals defects used on the XICS spectrometer on the Ar XVII spectra is studied in WEST. An analytical diffraction pattern routine is used to highlight 2 issues causing a line-doubling effect on spectra: a miscut angle due to the manufacturing of crystals and ambient temperature changes. The combination of both leads to angular offsets of order of the millimeter, corresponding to the spectral offset between doubled lines on experimental spectra. On another hand, the configuration of the spectrometer makes it possible to evaluate electron temperature profiles and to reveal the presence of spectral lines of Tungsten ionic species creating discrepancies between 2 intensity line ratios used, the He-like Ar resonance line w to $i/$ the Li-like Ar dielectronic satellite line k and $ii/$ the $n \geq 3$ satellite lines.

Introduction: A 2D X-ray spectrometer equipped with spherically bent crystals is operated on the WEST tokamak [1]. 3 sets of Bragg Quartz crystals, targeting 3 ionic species (Ar XVII, Ar XVIII, Fe XXV), are mounted on a patented rotating table [2] permitting to switch remotely the crystal facing the plasma. Fig.1 presents the Ar XVII crystal made in 2 separate halves, as the other sets of crystals. This experimental set-up allows measurements of LOS-integrated profiles of: $i/$ the electron temperature based on measurements of line intensity ratios, the He-like Ar resonance line w ($1s^2 \ ^1S_0 - 1s2p \ ^1P_1$) to the Li-like Ar dielectronic satellite k ($1s^2 2p \ ^2P_{1/2} - 1s2p^2 \ ^2D_{3/2}$) and to the $n \geq 3$ satellite lines ($1s^2 \ nl - 1s2p \ nl$), $ii/$ the ion temperature based on the Doppler broadening and $iii/$ the plasma velocity on the Doppler shift. The crystals manufacturing in 2 halves induce different structural properties and especially different miscut angles, a parallelism defect between the optical surface and the reticular planes. This issue has induced a line-doubling on the spectra for the C3 and C4 plasma campaigns. Studying these data will help us to better characterize the influence of crystal properties on experimental data. From the last C5 campaign, 1 half has been masked in order to improve the spectral resolution, thus allowing to emphasize the difference with the previous campaign and to reconstruct the first LOS-integrated T_e profiles.

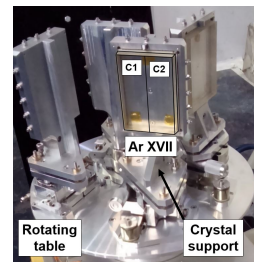


Figure 1: Top-view picture of the rotating table on which are placed the crystals sets.

Experimental set-up and Ar XVII spectra: The spectrometer is installed in a Johann configuration, permitting to focus photons towards the same image on the detector, for a resolving spectral power of $\lambda/\Delta\lambda \approx 10^5$, and to spatially resolve the LOS-integrated spectra. The crystals used are called Bragg crystals because they act as mono-chromatic and mono-angular mirrors, following the Bragg relation : $n\lambda = 2d_{hkl}.\sin(\theta_B)$. This equation, where λ ,

d_{hkl} and θ_B are respectively the photon wavelength, the inter-reticular spacing and the Bragg angle of reference, gives the condition of diffraction of X-rays from which constructive interferences occur.

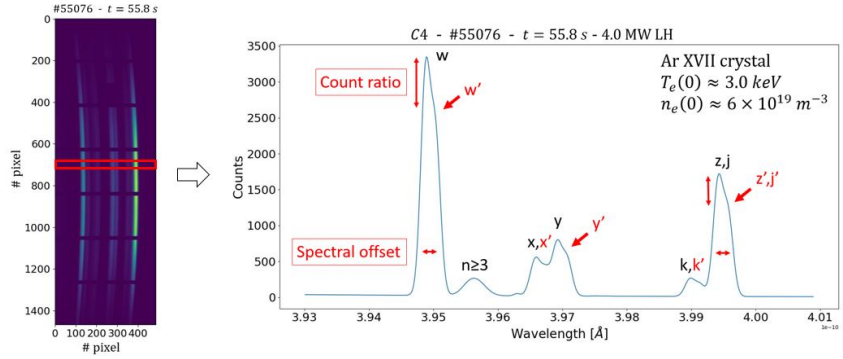


Figure 2: Line-doubled Ar XVII spectrum from C4 plasma campaign.

A 2D camera is used to record an image of the photon count per pixels. Fig. 2 shows an example of the spectra images available, for the C4 campaign, and an extracted spectra from the camera center. The intrinsic He-like and Li-like Argon spectral lines are recognizable but also a line-doubling effect on all the lines and characterized by a spectral offset and a doubled line intensity, or count, ratio. This issue is mainly due to the manufacturing of the crystals in 2 halves. The aim is to understand both the causes and effects of this line-doubling effect. The focus is made here of the spectral offset, entirely due to the crystals defects.

Numerical diffraction profiles: In order to better understand the diffracting properties of such crystals, we can compute analytically their diffraction power [3] and obtain a diffraction pattern, or rocking curve, describing the variations of the power ratio. The power ratio represents the intensity ratio between the diffracted and incident beams, for a given spectral line versus a range of angles of diffraction around the Bragg angle of reference. It occurs that the maximum power ratio is always lower than 1 due to absorption processes within the crystal and slightly shifted from the Bragg angle of reference by few arcsecs. Thanks to the literature, 2 issues have been identified affecting the diffraction pattern and inducing 2 dominant different angular offsets: i/ a miscut angle α between the optical surface and the reticular planes inducing a geometrical defect $\Delta\theta_1^\alpha$ and ii/ an ambient temperature change inducing a variation of the d_{hkl} inter-reticular spacing $\Delta\theta_3^T$ [4].

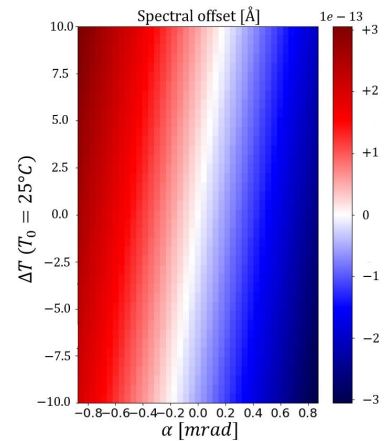


Figure 3: 2D map of the computed angular offset versus $\Delta\theta_1^\alpha$ and $\Delta\theta_3^T$ variations

Both have the same order of magnitude of offset as shown in Fig. 3. The maximum spectral offset of the diffraction pattern induced by their combination rise up to $\approx 3m\text{\AA}$. Thanks to these computations, the parallelism defect and the d_{hkl} variations are identified as the main angular offset components. The aim now should be to compare these results to what is fitted from experimental data.

Modelling lines on XICS synthetic diagnostic: Coupling the computed power ratio per angle with a ray-tracing routine on the XICS synthetic diagnostic, we can determine the positions of a given spectral line diffracted by both Ar XVII half-crystals modelled and study the offset induced. As shown in Fig. 4, affecting to them a temperature change of 10°C and miscut angles of $\alpha^{C1} = 1 \text{ arcmin}$ and $\alpha^{C2} = 0 \text{ arcmin}$, the computed pixel offset is about 1.5 mm when for the doubled resonance line w showed, the same order of magnitude have been determined. The offset is also very close to the natural spectral gap between the 2 inter-combination satellite lines x and y (Fig. 2). The combination of these 2 issues is fully sufficient to explain the spectral offset. Another important point, having the control on the ambient temperature affecting the crystals, and given the lack of accurate determination of the miscut on the crystals, we could possibly attenuate, or amplify, the effects of the latter, as Fig. 3 suggests. Despite the identification of causes for the spectral offset, none of the issues presented here seem to be among those responsible for the doubled line intensity ratio.

Electron temperature profiles: Now, looking at C5 campaign data, we can compute the LOS-integrated w/k and $w/n3$ line ratios and use it as a LOS-integrated proxy of the electron temperature profiles. Fig. 5 shows 2 spectra recorded during 2 consecutive heating phases: the Ohmic phase with up to 0.5MW power (in blue line) and the LHCD with up to 4.5MW of LH power (in red line) for this specific plasma shot. We can notice the presence of the intrinsic spectral lines from the Ar XVII crystals and some additional spectral lines which have been identified from [5] due to W^{43+} and W^{44+} , that typically appear above $T_e \geq 1.8 - 2\text{keV}$. One of them is located very close to the line k at 3.9898\AA , thus inducing potential errors on its total intensity record. The associated electron temperature profile in Fig. 5 is compared with

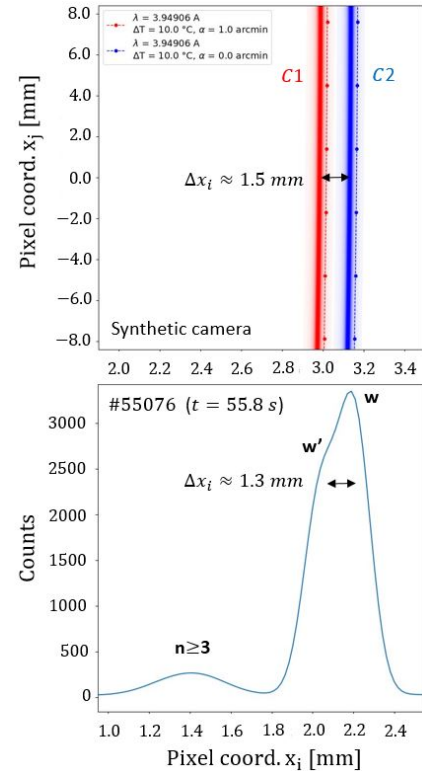


Figure 4: Comparison between modelled w line on synthetic camera and pixel offset on experimental data.

another line ratio $w/n3$ during both heating phases. These profiles are varied along a coordinate ρ representing the normalized plasma height associated to each LOS. During the Ohmic phase, the electron temperature is found to be constant in the plasma core, $-0.2 < \rho < 0.2$.

During the LHCD phase, the $w/n3$ profile reaches a maximal temperature at the very plasma center of 2.7 keV while the w/k profile is saturating at 1.8 keV. This is explained by the presence of a polluting

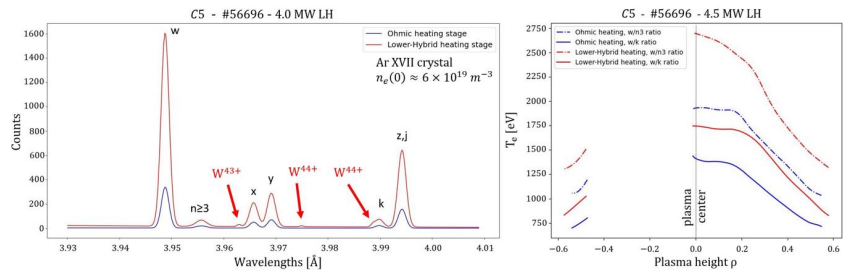


Figure 5: Spectra from Ar XVII w/o line-doubling polluted by ionic W spectral lines and comparison of intensity line ratios for the T_e profiles.

W line next to the k line, increasingly misleading the fit routine as the measured intensity for this spectral line increases. On the contrary, no polluting W line have been recorded next to the n3 lines, defining the $w/n3$ ratio the most trustful to estimate electron temperatures inside the plasma for now.

Conclusion: During the C3 and C4 campaigns, both Ar XVII half-crystals were used and induced a line-doubling issue on spectra, characterized by a spectral offset and a doubled line intensity ratio. The former is mainly due to a miscut angle different in each half-crystal and to an ambient temperature change affecting its inner lattice, causing at least offsets of $3m\text{\AA}$. The combination of both is good enough to explain the spectral offset fitted on experimental data. In parallel, studying their effects on diffraction patterns of Quartz crystal, no apparent decrease of intensity diffracted have been noticed, excluding them from the list of possible causes for the doubled line intensity ratio. Furthermore, masking 1 half-crystal allows to recover a satisfactory spectral resolution but at high temperatures, W^{44+} spectral lines pollute the spectrum, thus invalidating the w/k line ratio for the T_e estimation. In WEST upcoming campaigns, efforts will be made to accurately identify all the polluting spectral lines but also to acquire new experimental data, exchanging the position of the masks on half-crystals, in order to identify the causes of the doubled line intensity ratio issue.

References

- [1] D. Vezinet et al., ECPD conference; Lisboa, 2019, poster P3.6
- [2] G. Colledani, patent number 1653710 from the 27th April 2016
- [3] R. Bartiromo, F. Bombarda et al., Nucl. Instrum. Methods Phys. Res. A **221**, 453 (1984)
- [4] L. Delgado-Aparicio et al., Plasma Phys. Control. Fusion **55**, 125011 (2013)
- [5] J. E. Rice et al., J. Phys. B: At. Mol. Opt. Phys. **54**, 095701 (2021)